Materials Chemistry and Physics 212 (2018) 230–236

Contents lists available at ScienceDirect

Materials Chemistry and Physics

journal homepage: www.elsevier.com/locate/matchemphys

Coexistence of spin-lattice and spin-spin relaxation mechanism in perovskite manganite $(La_{0.5}Pr_{0.5})_{0.67}Ca_{0.33}MnO_3$

Lili Chen [a], Jiyu Fan [a, *], Yu-E. Yang [a], Fengjiao Qian [a], Dazhi Hu [a], Jindong Liu [a], Yanda Ji [a], Wei Tong [b], Langsheng Ling [b], Lei Zhang [b], Li Pi [b], Yuheng Zhang [b], Hao Yang [a]

[a] Department of Applied Physics, Nanjing University of Aeronautics and Astronautics, Nanjing 210016, China
[b] Anhui Key Laboratory of Condensed Matter Physics at Extreme Conditions, High Magnetic Field Laboratory, Chinese Academy of Sciences, Hefei 230031, China

HIGHLIGHTS

- An obvious phase separation in LPCMO was confirmed by EPR.
- We find two spin relaxation mechanisms in LPCMO.
- The inhomogeneity of the phase transition region can be disclosed by the asymmetry factor of EPR spectrum.

ARTICLE INFO

Article history:
Received 7 May 2017
Received in revised form
30 December 2017
Accepted 8 March 2018
Available online 10 March 2018

Keywords:
Magnetic materials
Magnetic transitions
Electron resonance

ABSTRACT

Electron paramagnetic resonance (EPR) was applied extensively to probe the phase separation and spin relaxation mechanism in the perovskite manganites. In this study, we conducted the measurement of EPR for the perovskite manganites $(La_{0.5}Pr_{0.5})_{0.67}Ca_{0.33}MnO_3$. We found that both paramagnetic and ferromagnetic resonance peaks simultaneously emerged on resonance spectrum near below T_C, exhibiting a typical characteristic of phase separation. The linewidth of EPR spectrum progressively enlarged upon the rising of temperature in the temperature range of $T > T_C$ and a quasilinear variation of peak-peak width was observed at $T_C < T < 500$ K. In contrast to the usual beliefs that the variation of peak-peak linewidth can be understood either by spin-lattice relaxation or by spin-spin relaxation, however, the linewidth behavior observed here shows a coexistence of two spin relaxation mechanisms. We proposed that the inhomogeneous electronic phases due to the intrinsic self-organizing growth were responsible for the appearance of multiple spin exchange interactions and variational relaxation mechanism. This finding would be possible to pave a new way for further investigating magnetic correlations and spin dynamics in the paramagnetic hole-doped manganites.

1. Introduction

Phase separation(PS), namely, the simultaneous presence of two different submicrometer magnetic regions, has attracted much attention in perovskite manganites $R_{1-x}A_xMnO_3$ (R = rare earth element, A = divalent alkaline earth element) due to its important role in understanding the unique physical properties of these compounds, e.g., colossal magnetoresistance effect, ferromagnetic insulating state, coexistence of ferromagnetic state and charge ordering phase [1–4]. Not only that, studies of PS are also helpful for clarifying the fundamental physics of strong electronic interactions in these complex oxides because PS originates from strong coupling between spin, charge, orbital, and lattice degrees of freedom [5–8]. Uehara et al. directly probe and observe the PS behavior (the separation of charge ordering phase and ferromagnetic region) in $(La_{1-y}Pr_y)_{5/8}Ca_{3/8}MnO_3$ using magnetic force microscopy [9]. Scanning tunneling spectroscopy, another powerful tool to study PS, was carried out to reveal the coexistence of insulating and metallic region in single crystals $La_{0.7}Ca_{0.3}MnO_3$[10]. Recently, the legible morphology of refined PS evolution in $La_{0.67}Ca_{0.33}MnO_3$ film has been also reported [11]. Hitherto, although numerous studies have been carried out to understand PS,

* Corresponding author.
E-mail addresses: jiyufan@nuaa.edu.cn (J. Fan), weitong@hmfl.ac.cn (W. Tong), yanghao@nuaa.edu.cn (H. Yang).

https://doi.org/10.1016/j.matchemphys.2018.03.027
0254-0584/

the intrinsic reason for the PS remains unclear.

Besides the above methods, EPR is also an effective technology to prob the PS in perovskite manganites. Deisenhofer et al. reported that the FM clusters embedded in paramagnetic phase of $La_{0.875}Sr_{0.125}MnO_3$ single crystals with the utilization of EPR [12]. Moreover, because EPR is also a powerful tool to study the magnetic correlations and spin dynamics of manganites at microscopic level, many EPR work have been performed to elucidate their interactions between spin and charge degrees of freedom which is based on the valuable information obtained from the temperature dependence of EPR spectra parameters, e.g., line shape, effective g-factor, peak-to-peak linewidth ΔH_{PP} and double integrated intensities(DIN). At present, how to rightly understand the peak-to-peak linewidth ΔH_{PP} dependency on temperature is being mostly debated and a consensus on the relaxation mechanism remains elusive in this area. Some different mechanisms have been suggested to interpret a linear variation of ΔH_{PP} vs T above T_C which is a pervasive characteristic for a wide variety of mixed-valent manganites. By and large, according to different relaxation mechanisms, the main controversy focused on two opposite viewpoints. One is spin-lattice relaxation suggested by Shengelaya et al. whereas the other is spin-only relaxation proposed by Hubei and Causa et al. [13–15].

In general, the EPR signal of the doped manganites was referred to the contribution of Mn^{4+} ions instead of Mn^{3+} ions owing to a large zero-field splitting and very short spin-lattice relaxation in the Jahn-Teller Mn^{3+} ions [16]. According to the first viewpoint, the energy transfer is provided by thermoactivated hopping of the small polarons related with jumps of e_g electrons from Mn^{3+} to Mn^{4+} ions. Therefore, Shengelaya et al. utilized spin-lattice relaxation (the so-called "bottleneck model") to interpret the observed similarity of the temperate dependence of linewidth ΔH_{PP} and that of the polaron hopping conductivity in $La1_{1-x}Ca_xMnO_3$ [13]. On the contrary, considering a fact that the main interaction determined in manganites is due to spin-spin exchange coupling between the Mn^{3+} and Mn^{4+}, Causa et al. [14] proposed that Mn^{4+} and Mn^{3+} ions all contributed to EPR signal but without any spin-polaron exchange process. This viewpoint (spin-only relaxation mechanism) is supported from the amazing consistency between the theoretical calculation and the experimental observation of resistivity dependence on temperature in $La_{0.67}Ca_{0.33}MnO_3$ which is measured upon to very high temperatures [14,15]. In addition, according to Huber's theory and some related experimental results, Rozenberg et al. proposed the spin-spin relaxation was appropriate only for electron-doped/pristine manganite whereas the carrier-lattice relaxation plays key role in hole-doped manganite. [17], Therefore, to resolve these debates, it is well worth further studying the linewidth variation and the spin relaxation mechanism in perovskite manganites.

In this study, we presented a detailed investigation of magnetic properties and the analysis of EPR spectrum for the manganite $(La_{0.5}Pr_{0.5})_{0.67}Ca_{0.33}MnO_3$ (LPCMO). Our results show that a paramagnetic-ferromagnetic (PM-FM) transition occurs at 131.5 K and its ground state is of FM state. A coexistence of PM phase and FM phase was clearly observed at the temperature ranging from 125 to 90 K based on the EPR spectrum, thereby indicating that there was a noticeable PS characteristic. In contrast to the majority of reported results, a quasilinear variation of temperature dependency of EPR linewidth can be understood by both spin-lattice and spin-only relaxation mechanism. We think that the local chemical inhomogeneous induce the various types of carries which are responsible for the coexistence of multiple spin exchange interactions in system. This finding suggests novel pathways for understanding the underlaying relaxation mechanism and complex magnetic interaction in perovskite manganite.

2. Experimental

A polycrystalline LPCMO sample was prepared using traditional solid state reaction method [18]. The structure and phase purity of the as-prepared sample were checked by powder X-ray diffraction (XRD) using Cu Kα radiation at room temperature. The magnetization versus temperature and magnetic field were measured using a Magnetic Property Measurement System (Quantum Design MPMS 7T-XL) with a superconducting quantum interference device (SQUID) magnetometer. The EPR measurements were obtained for the powder samples at selected temperatures using a Bruker EMX-plus model spectrometer with a heater operating at X-band frequencies ($\nu \approx$ 9.4 GHz).

3. Results and discussion

Fig. 1 shows the structural refinement of the XRD data obtained for the polycrystalline perovskite manganite LPCMO using the Rietveld method (using Fullprof program). The XRD patterns proved that the sample was pure and a single-phase of orthorhombic structure with space group Pnma. Refinement of the XRD data gives the following reliability factors: the weighted factor $R_{wp} = 8.16\%$, $Rp = 7.29\%$, and the structure factor 2.16%. Based on the Rietveld refinements, the lattice parameters a, b, and c are found to be 5.463 Å, 7.7085 Å, and 5.457 Å, respectively. Therefore, the fitting results in Fig. 1 confirm the high quality of the LPCMO sample for the investigation in this study.

Fig. 2 (left-hand axis) shows the temperature (T) dependence of magnetization (M) measured under an applied magnetic field of H = 100 Oe. One sharp PM-FM phase transition occurs at the Curie temperature T_C~131.5K which is determined from the differential M(T) curve. Right-hand axis shows the inverse susceptibility X^{-1} vs T. Obviously, a linear variation of $X^{-1}(T)$ curve indicates that the evolution of susceptibility dependency on temperature can be preferably described by the Curie-Weiss law at PM region, i.e. $\chi = \frac{C}{T-T_\theta}$, where T_θ is the Curie-Weiss temperature and C is the Curie constant defined as: $C = \frac{N_A}{3k_B}(P_{eff}^{exp})^2$, N_A is the number of Avogadro, k_B is Boltzmanns constant, and P_{eff}^{exp} is the experimental effective moment. A linear fit to high temperature yields the Curie constant (C = 3.984 emu K/mole Oe)) and the Curie-Weiss temperature $T_\theta = 150$ K. The positive value of T_θ confirms the existence of FM exchange interaction in this sample. Based on the data of the Curie constant obtained from the fitting, the effective PM moment

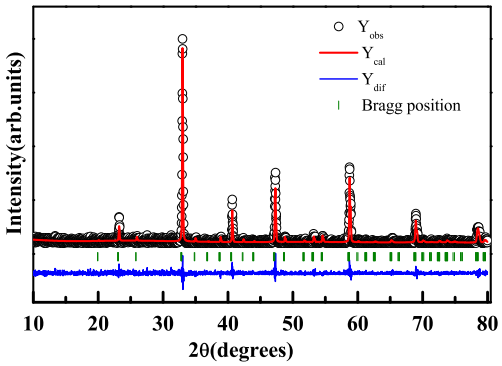

Fig. 1. (Color online) Powder XRD patterns obtained for $(La_{0.5}Pr_{0.5})_{0.67}Ca_{0.33}MnO_3$. Black circles: experimental data. Red line: calculated pattern. Olive ticks: positions of the Bragg reflections for the main phase. Blue line: difference between the experimental and calculated patterns. (For interpretation of the references to colour in this figure legend, the reader is referred to the Web version of this article.)

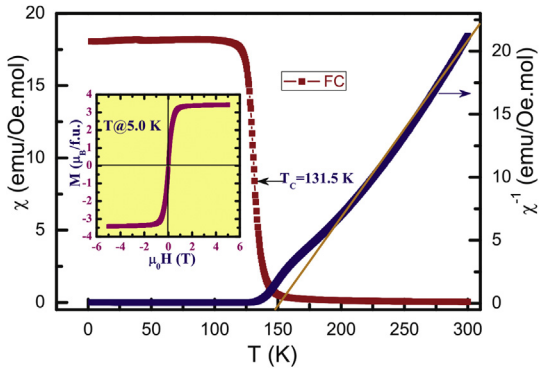

Fig. 2. (Color online) Left axes: Temperature dependence of magnetic susceptibility χ for $(La_{0.5}Pr_{0.5})_{0.67}Ca_{0.33}MnO_3$ measured under an applied field of 100 Oe; Right axes: Temperature dependence of inverse susceptibility X^{-1} and the solid line represents the linear fitting according to Curie-Weiss law; Inset shows the plot of isothermal magnetization measured at 5.0 K. (For interpretation of the references to colour in this figure legend, the reader is referred to the Web version of this article.)

($P_{eff} = 2.83\sqrt{C}$) is determined to be $P_{eff} = 5.65\ \mu_B$. The theoretical paramagnetic effective moment(μ_{eff}^{the}) of LPCMO sample could be deduced according to the following relation [19].

$$\mu_{eff}^{the^2} = 0.335 g_{Pr^{3+}}^2 J_{Pr^{3+}}(J_{Pr^{3+}}+1) + 0.67 g_{Mn^{3+}}^2 J_{Mn^{3+}}(J_{Mn^{3+}}+1) + 0.33 g_{Mn^{4+}}^2 J_{Mn^{4+}}(J_{Mn^{4+}}+1) \quad (1)$$

where g is the Lande factor and J=(L + S) is the total angular moment. For Mn^{3+}/Mn^{4+} ions, we have J = S due to the absence of orbital moment. Here, the spin-only moment of the free ions Pr^{3+}, Mn^{3+}, and Mn^{4+} are 3.58, 4.90, and 3.87μ_B, respectively. Based on Eq. (1), we obtained the theoretical moment μ_{eff}^{the} was equal to 5.032μ_B, which was basically close to the experimental effective moment μ_{eff}^{exp} of 5.65μ_B.

The inset of Fig. 2 shows the isothermal M(H) curve measured at 5.0 K. The magnetization increases sharply and then tends to saturation as the applied magnetic field approaches to $\mu_0 H = 0.8$ T, indicating the ground state is of FM phase. Here, the saturated magnetization (M_S) can be obtained from an extrapolation of the high field M(H) curve to $\mu_0 H = 0$, and the value of $M_S = 3.42\ \mu_B$ is determined. According to Rhodes-Wohlfarth criterion [20], the degree of itinerancy can be determined from the ratio of P_{eff} to M_S. The ratio is close to one for the localized moment whereas it is larger than one for the itinerant moment. Here, the ratio of 1.65 implies that the LPCMO electrons possess an itinerant character.

In general, for the PM state of an isotropic magnetic system, its EPR spectrum usually shows as a differential Lorentzian curve. Two typical EPR spectrum of LPCMO sample were plotted in the inset of Fig. 3(a). One is measured at 300 K and the other is measured at 200 K. Both of them are far above $T_C = 131.5$ K and the system is in the PM phase. As $T < T_C$, a strong FM resonance peak occurs at the low field regime and replaces the previous PM resonance peak since that the generation of FM phase enhances its inner magnetic field. Fig. 3(a) shows the EPR spectrum measured from 125 to 90 K. Clearly, in contrast to the general characteristic of FM resonance, there are two resonance peaks rather than a single peak at the same temperature in Fig. 3(a). The left peak of the low field region is FM peak whereas the right peak of high field region is PM peak. This means that two different magnetic states coexist in the temperature region of 90 < T < 125 K, showing as a typical characteristic of PS. Similarly, in the compound $(La_{0.4}Pr_{0.6})_{0.67}Ca_{0.33}MnO_3$[21], such a PS behavior has been also reported.

As is well-known, the double-exchange (DE) interaction between Mn^{3+} and Mn^{4+} are mainly responsible for a strong PM-FM phase transition in the doped perovskite manganites. Normally, in a fully homogeneous DE system, one would expect a pure FM phase below T_C. Here, the appearance of PS behavior implies a considerable inhomogeneity in the current LPCMO sample. In order to testify this conjecture, we study the asymmetry factor (A/B, see inset of Fig. 3(b)) of the measured EPR spectrum below 300 K. Before performing the measurement in this work, the LPCMO bulk was first pulverized to make it become a perpusillus powder. Thus, the asymmetric PM signal due to the effect of the shape anisotropy and selectional distribution of PM orientation can be effectively avoided. Fig. 3(b) shows the variations of asymmetry factor as a function of temperature. If the deviation no more than 1% can be thought as a regular error, the deviation larger than 1% should be referred to an existence of inhomogeneity. As shown in Fig. 3(b), at the range of 180 K < T < 300 K, all the values of A/B are intermediate between two yellow imaginary line where the deviation value corresponds to ±1%. Based on the previous consideration, it is concluded that the sample is in homogeneous PM state as T > 180 K. Conversely, at T < 180 K, the value of asymmetry factor shows a sharp increase and significantly displaces from the center of regular error. The variations of asymmetry factor imply the existence of inhomogeneity. In fact, the asymmetry factor deviated from regular error is also consistent with the $X^{-1}(T)$ curve which deviates from the Curie-Weiss law just at 180 K in Fig. 2. Both behaviors occurred at the same temperature further indicate the existence of PS (FM phase separates from PM phase) in LPCMO sample.

Apart from the discussion of PS, we turn to study the magnetic behavior in the temperature region of $T > T_C$ where the sample is in PM state. In order to clarify the relaxation mechanism, the EPR spectrum were measured up to the temperature of 500 K. As shown in Fig. 4, a series of single EPR resonance lines with a differential Lorentzian shape (dP/dH) were observed. The resonance position is almost at $\mu_0 H = 0.33$ T. The inset shows the magnified plot of EPR spectrum from 170 to 130 K. Obviously, the EPR spectrum exhibits a remarkable shift only from 130 K, in agreement with the PM-FM phase transition observed on M(T) curve at 131.5 K. The magnetic coupling intensity can be reflected from the change in effective g-factor, which can be calculated from the resonance field formula $g = h\nu/\mu_B H_{res}$ (h is the Plank constant; ν is the frequency of microwave; μ_B is the Bohr magnetor). Fig. 5 plots the variation of g-factor dependence on temperatures. It is found that the g-values are nearly temperature independent except for those close to T = 300 K. In the PM region, the free electron value g_e is about ~2.0023. In the previous work, Rao et al. reported that there was a universal feature in manganites in which the g-value for the hole-doped sample is more than g_e whereas it is less than g_e for the electron-doped one at room temperature [22]. Here, the variation of g-values in Fig. 5 is basically consistent with this one feature. Above T_C, the g-values slowly increase with the decrease of temperature. Below T_C, the g-values increase dramatically from 2.1 to 2.34 but shift to decrease from T = 115 K. In order to reflect this variation more clearly, the inset of Fig. 5 presents the absorption spectrum as a function of field in some representative temperatures. Obviously, the peak of resonance field gradually shifts to low field regime as temperature decreases from 350 to 130 K. The variations of g-factor can be understood from the enhancement of the spin-orbit coupling constant and the orbital ordering when the temperature approaches the point of PM-FM phase transition from high temperature. These variations directly influence the crystal field splitting and hence can result in a rising of g-factor. In fact, the orbital ordering associated with PM-FM phase transition has been widely testified by many neutron scattering experiments [23,24].

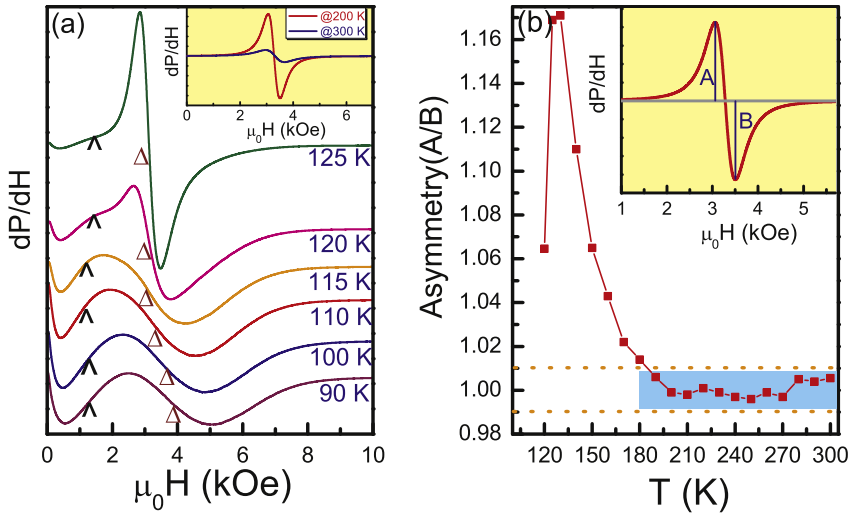

Fig. 3. (Color online) (a) EPR spectrum of $(La_{0.5}Pr_{0.5})_{0.67}Ca_{0.33}MnO_3$ at temperatures of 125 K⩾T⩾90 K and inset show two representative paramagnetic resonance curves at 200 and 300 K; the marks "∧" and "△" denote the position of the ferromagnetic and paramagnetic signals, respectively. (b) Asymmetry factor (A/B) dependence of temperature and two dashed lines represent the deviation of ±1%; Inset shows the low and high field maximum value (A and B) of ESR signals. (For interpretation of the references to colour in this figure legend, the reader is referred to the Web version of this article.)

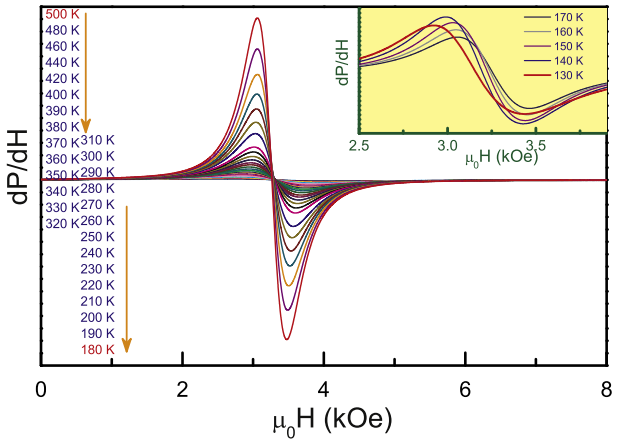

Fig. 4. (Color online) EPR spectrum of $(La_{0.5}Pr_{0.5})_{0.67}Ca_{0.33}MnO_3$ at temperatures of 180 K⩽T⩽500 K; Inset shows the magnified EPR spectrum at 130 K⩽T⩽170 K. (For interpretation of the references to colour in this figure legend, the reader is referred to the Web version of this article.)

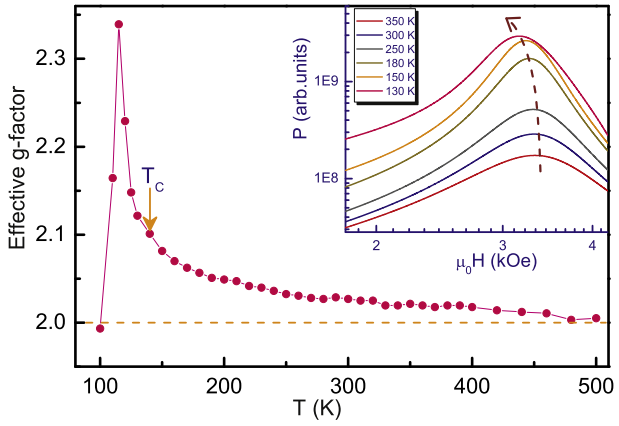

Fig. 5. (Color online) Effective *g*-factor as a function of temperature; Inset shows the absorption spectrum as a function of field at some selected temperatures. (For interpretation of the references to colour in this figure legend, the reader is referred to the Web version of this article.)

Fig. 6(a) shows the temperature dependence of the EPR peak-peak width (ΔH_{PP}) which is defined as the width between the highest point and the lowest one in the EPR spectrum for LPCMO sample. One minimum linewidth occurs in 140 K whereas the ΔH_{PP} increases as temperature below and above T_C. Obviously, a quasi-linear variation of EPR linewidth occurred at $T > T_{min}$ is a universal nature for the hole-doped perovskite manganites. In general, the broadening of EPR linewidth arises from shortening of spin-lattice relaxation time at $T > T_C$ due to the hopping of e_g electrons via spin-orbit coupling whereas from the formation of spin cluster glass state at $T < T_C$ where some magnetic moments are frozen. So far, for the most of hole-doped manganites, the conduction mechanism of PM regime is extensively studied with the adiabatic small polaron hopping model. Considering that a similar behavior between temperature dependence on EPR linewidth and conductivity has been found [13], Shengelaya et al. proposed a so-called "bottleneck model " to describe the ΔH_{PP} vs temperature by using the following formula [25]:

$$\Delta H_{PP}(T) = \Delta H_0 + \frac{A}{T} exp(-E_a/k_B T) \quad (2)$$

where A is a constant and E_a is the activation energy for small polaron hopping. Meanwhile, the activation energy E_a can be obtained from fitting data by Eq. (2). Fig. 6(b) plots the $\ln(\Delta H_{PP} T)$ vs 1000/T and the straight line represents the fitting results. The activation energy E_a is 71.57 meV. As for the hole-doped manganites, the conductance is achieved by the e_g electronic hoping. Therefore, the relaxation of exchange coupled localized spins (Mn^{4+}) to the lattice occurs via conduction electrons (Mn^{3+}). Due to lattice distortion, the mobility of e_g electron is reduced resulting in the localization of carriers and the formation of polaron. Here, the substitution of Pr^{3+} ion on A-site sublattice exacerbates lattice distortion giving rise to the formation of polaron. Thus, the spin-lattice relaxation mechanism is suitable for describing the quasi-linear variation of EPR linewidth dependence on temperature for LPCMO sample.

Besides the g-factor and peak-width ΔH_{PP}, the intensity of EPR

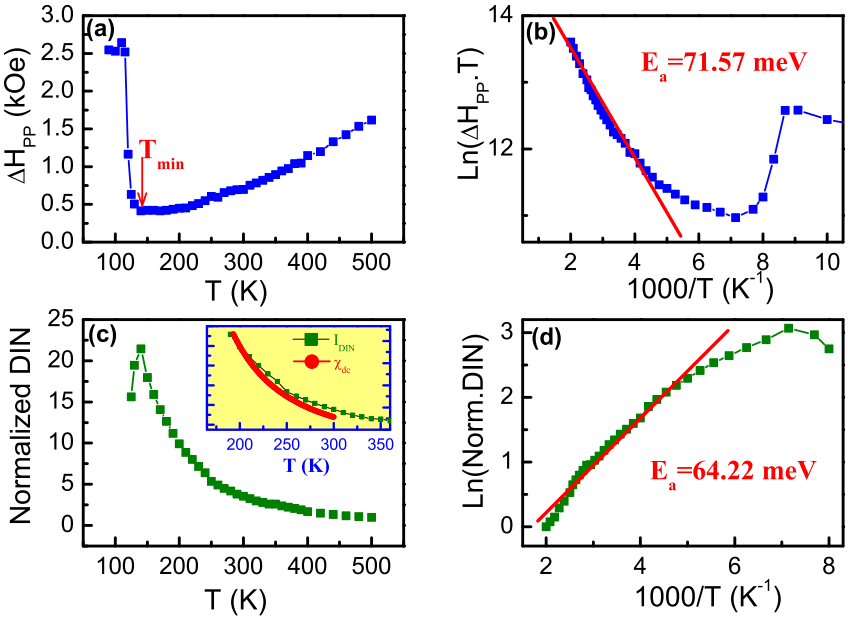

Fig. 6. (Color online) (a) EPR linewidth ΔH_{PP} vs T; (b) EPR linewidth plotted as $\ln(\Delta H_{PP}T)$ vs 1000/T (the solid line represents the fitting results with equation (1)); (c) Temperature dependence of the double integrated intensity DIN(Inset represents the EPR intensity I_{EPR}(solid squares) and X_{dc} (solid circles) vs T at different temperatures.); (d) Arrhenius plots of DIN and the solid line represents the fitting results with equation (3). (For interpretation of the references to colour in this figure legend, the reader is referred to the Web version of this article.)

spectra is also an important parameter to provide some information about the magnetic correlations of material. Generally, the intensity of EPR spectra can be calculated by the double integration of EPR spectra (dP/dH). Fig. 6(c) presents the results of the normalized double integrated intensities (DIN). Similar to the variation of g-factor, the value of DIN progressively enlarged as for the development of FM ordering with the decrease of temperature but decreased from T = 140 K. For comparison with magnetization of PM region, the inset of Fig. 6(c) shows the EPR intensity (I_{EPR}) and the dc magnetic susceptibility (X_{dc}) versus temperature. Clearly, the variation of I_{EPR} basically agrees with the variation of X_{dc}(T), indicating that the magnetic variations detected from EPR spectra are in perfect accordance with the results obtained from magnetization measurements. In PM region, the EPR intensity is usually described by the thermally activated model(the Arrhenius law) [14,26]:

$$DIN(T) = I_0 exp(E_a/k_B T) \tag{3}$$

where E_a is the activation energy for dissociation of paramagnetic spin clusters. As show in Fig. 6(d), the activation energy was deduced to be 64.22 meV, which is very close to the value deduced from the temperature dependence of EPR linewidth (E_a = 71.57 meV). Both values are at the range of the typical activation energy (50–100 meV) for small polarons hopping in PM manganites [27,28]. Here, a similar result obtained from two independent methods reflects the existence of polarons hopping above T_C. Therefore, it is reasonable that the quasilinear variation of peak-peak width observed in LPCMO sample is attributed to the spin-lattice relaxation mechanism.

In fact, for PM EPR linewidth, the quasilinear variations of peak-peak width dependence on temperature can been also explained by spin-spin relaxation mechanism. Huber et al. proposed that the EPR linewidth was determined by spin-spin interaction rather than spin-phonon (lattice) exchange interaction. It was suggested that approaching T_C from higher temperatures gives rise in lengthening the relaxation time and correlation length of critical region due to the development of FM ordering. This results in a narrower EPR linewidth at critical region compared with that in high temperature region. The strong support for this viewpoint comes from the amazing agreement between their theoretical calculation and experimental results [15]. Here, we also need to clarify whether there are some possible applicability to understand the quasilinear EPR linewidth in Fig. 6(a) by the spin-spin relaxation mechanism. According to Hubei's theory, the linear dependence of linewidth is attributed to critical and non-critical contributions. Both contributions for the linewidth can be written with

$$\Delta H_{pp}(T) = \frac{\hbar[c + f(\varepsilon)]}{g\mu_B T\chi_0} \tag{4}$$

where $f(\varepsilon)$ is the critical contribution to ΔH_{PP} from spin-spin coupling, which is significant only for $\varepsilon = (T-T_C)/T_C \leqslant 0.1$ and c is non-critical contribution to ΔH_{PP} from spin-lattice (phonon) interactions for $T \gg T_C$. Here, we mainly consider the PM region where the temperature is $T \gg T_C$. Thus, the second term $f(\varepsilon)$ in the nominator of Eq. (4) can be ignored and Eq. (4) is simplified as:

$$\Delta H_{pp}(T) = \Delta H_{PP}(\infty)\frac{C}{T\chi} \tag{5}$$

where χ is the measured paramagnetic susceptibility and $\Delta H_{PP}(\infty)$ is the linewidth expected at temperature high enough. For comparison, the value of $\Delta H_{PP}(\infty)$ for LPCMO and some relate manganites are summarized in Table 1. Obviously, the value of $\Delta H_{PP}(\infty)$ =

Table 1
Values of $\Delta H_{PP}(\infty)$ for manganite with different percentage of Mn^{3+}/Mn^{4+}

Composition	Ref.	$\Delta H_{PP}(\infty)$ (Oe)
$(La_{0.5}Pr_{0.5})_{0.67}Ca_{0.33}MnO_3$	this work	1617
$La_{0.5}Ca_{0.5}MnO_3$	[15]	1600
$La_{0.67}Ca_{0.33}MnO_3$	[14]	2400
$CaMnO_3$	[15]	1050
$LaMnO_3$	[35]	2600

1617 Oe is within a reasonable and normal range. Due to the spin-phonon interactions (vibrations of the lattice) dependence on the variation of temperature, if there is no contribution to the linewidth from spin-phonon interactions, the product $\Delta H_{PP}T\chi$ should be a temperature independent constant. Namely, in this case, it must be spin-spin relaxation rather than the spin-lattice relaxation which contributes to the PM linewidth. Fig. 7(a) shows the product $\Delta H_{PP}T\chi$ as a function of temperature above T_C. A horizontal line observed at $T > 150$ K clearly indicates that the value of $\Delta H_{PP}T\chi$ is independence on temperature. Obviously, this result completely contradicts the foregoing analysis that it is the spin-lattice relaxation contributed to the PM linewidth in LPCMO sample.

In general, for the most of manganites, the spin relaxation can be understood by either of the two mechanisms mentioned above. Here, the coexistence of both relaxation mechanisms in one material implies that the multiple spin exchange interactions (spin-lattice, spin-spin) generate in LPCMO sample. As we know, the prototypical manganite $(La_{1-y}Pr_y)_{1-x}Ca_xMnO_3$ is a typical material of PS, in which the competition among the ferromagnetic metallic, charge ordered insulating and paramagnetic insulating phases brings multiphase coexistence over a board range of temperatures [29,30]. Here, $(La_{0.5}Pr_{0.5})_{0.67}Ca_{0.33}MnO_3$ is one of compositions of $(La_{1-y}Pr_y)_{1-x}Ca_xMnO_3$. We propose the following scenario to understand why there are multiple spin exchange interactions in LPCMO sample. Because the hole-doped manganites are apt to form an inhomogeneous distribution due to self-organizing growth, La^{3+} ions and Pr^{3+} ions respectively concentrate in different regions. Thus, some microclusters/domains are $La_{0.67}Ca_{0.33}MnO_3$ but others are $Pr_{0.67}Ca_{0.33}MnO_3$. Due to the inherent discrepancy for the cationic radius of La^{3+} and Pr^{3+}, their electronic structures and spin-lattice coupling are not the same. Their electronic transports may be realized by the thermal activation and/or small polarons hopping. Both are all frequently observed in PM region of the hole-doped manganites [31,32]. Nevertheless, at the moment we are unable to distinguish the regions whose carriers are electrons or small polarons. Further investigation is needed, both theoretical and experimental, to resolve this problem. However, the scenario suggested here clearly points out that LPCMO sample forms some different regime which possesses different spin exchange interaction. So, two kinds of spin relaxation mechanisms co-occur in this material.

Based on the above discussion of relaxation mechanisms, we can study the spin dynamics in LPCMO sample by calculating the spin relaxation time (τ). The spin relaxation rate T^{-1} is equal to $(2T_1)^{-1} + T_2^{-1}$, where T_1 is longitudinal relaxation time and T_2 is transverse relaxation time. Generally, the former (T_1) is difficult to be measured because the power of standard pulse is far from the requested values of microwave power level. Therefore, the value of T_1 is rarely discussed as well. Here, we mainly study the transverse relaxation time (T_2). In fact, the measuring of the EPR linewidth is only correlated with the transverse relaxation time. Their relation is represented as follows:

$$\tau_2 = \frac{2}{\sqrt{3}\gamma\Delta H_{PP}} \tag{6}$$

where γ is the electronic spin gyromagnetic ratio. As shown in the inset of Fig. 7(a), the transverse relaxation time T_2 increases from 0.04 to 0.16 ns with the decrease of temperature. The variation range of T_2 obtained in LPCMO sample is basically consistent with the previous reports on other manganite materials. As the temperature approaches T_C from higher temperatures, the FM coupling progressively develops and the FM correlations strengthen. As a result, the fluctuating internal field (H_i) is weakened and suppressed, which facilitates the enhancement of transverse relaxation time. On the other hand, according to "noncritical Huber law" [33], the transverse relaxation rate T_2^{-1} also satisfies the following relation:

$$\tau_2^{-1} \propto \frac{1}{T\chi_{dc}} \tag{7}$$

In order to further validate the obtained time T_2, the left and right axes of Fig. 7(b) respectively show the variation of T_2^{-1} vs temperature and the $1/(T\chi_{dc})$ vs temperature. Obviously, above 200 K, both lines basically overlap each other and show a uniform variation indicating that the transverse relaxation time τ_2 obtained above is accurate. Below 200 K, the separation of both lines is on account of the temperature which starts to approach the critical region. In fact, as shown in the inset of Fig. 7(a), the drastic decrease for the transverse relaxation time τ_2 from T = 140 K is completely consistent with the variation of the asymmetry factor (A/B) in Fig. 3(b). In such a region, with the development of FM correlations upon cooling, the system generally generates non-uniform magnetization due to the local chemical inhomogeneous in ceramic samples. Thus it causes the broadening lingwidth near below T_C. By contrast, the absences of the broadening lingwidth have been verified in high-quality single crystal ($La_{0.67}Sr_{0.33}MnO_3$ and $Pr_{0.67}Sr_{0.33}MnO_3$) with perfect surface [34].

4. Conclusion

In summary, the magnetic properties and spin relaxation mechanism have been investigated in the hole-doped manganite LPCMO. We find the sample shows a PM and FM phase separated state near below T_C. Above T_C, a quasilinear variation of peak-peak width of EPR spectrum, being a common characteristic of

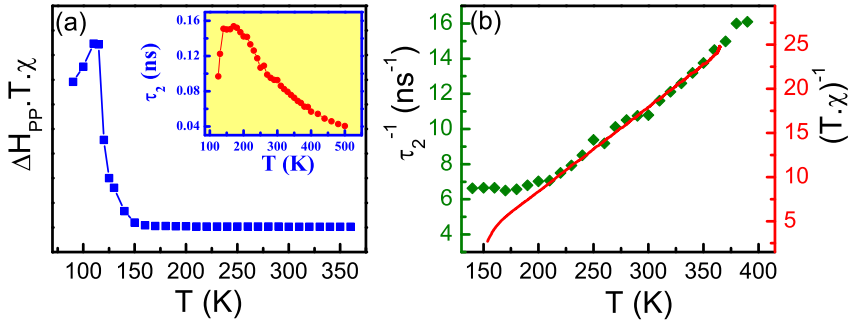

Fig. 7. (Color online) (a) Temperature dependence of the product $\Delta H_{PP}T\chi$ and inset shows transverse relaxation time (T_2) as a function of temperature; (b) Plots of transverse relaxation rate (T_2^{-1}) (left, solid square) and $(TX_{dc})^{-1}$ (right, solid line) dependence of temperature. (For interpretation of the references to colour in this figure legend, the reader is referred to the Web version of this article.)

manganite in PM region, has been observed until to 500 K. Different from the usual beliefs, this variation can be explained by two spin relaxation mechanisms, indicating the coexistence of spin-lattice and spin-spin relaxation in LPCMO material. We suggest that the existence of multiple spin exchange interactions mainly arises from the local chemical inhomogeneous which cause the formation of variational regime with different carries. Moreover, the deduced transverse relaxation rate T_2^{-1} also obeys "noncritical Huber law" in a wide temperature range, indicating the decrease of noncritical relaxation time due the weakness of FM correlation upon heating.

Acknowledgment

One of the authors Jiyu Fan would like to thank Prof. D. L. Huber for enlightening discussions. This work was supported by the National Key Research and Development Program of China (Grant No. 2017YFA0403502), the National Nature Science Foundation of China (Grant Nos. U1632122, 11774172, and 11574322), the Fundamental Research Funds for the Central Universities (Grant No. NE2016102, No. NP2017103, and NS2017052), and Foundation of Graduate Innovation Center In NUAA (Grant No.kfjj20160804).

References

[1] E. Dagotto, T. Hotta, A. Moreo, Phys. Rep. 344 (2001) 1.
[2] S. Jin, T.H. Tiefel, M. McCormack, R.A. Fastnacht, R. Ramesh, L.H. Chen, Science 264 (1994) 413.
[3] R. von Helmolt, J. Wecker, B. Holzapfel, L. Schultz, K. Samwer, Phys. Rev. Lett. 71 (1993) 2331.
[4] R. Mahendiran, S.K. Tiwary, A.K. Raychaudhuri, T.V. Ramakrishnan, R. Mahesh, N. Rangavittal, C.N.R. Rao, Phys. Rev. B 53 (1996) 3348.
[5] K. Khazeni, Y.X. Jia, Li Lu, Vincent H. Crespi, Marvin L. Cohen, A. Zettl, Phys. Rev. Lett. 76 (1996) 295.
[6] A.P. Ramirez, J. Phys. Condens. Matter 9 (1997) 8171.
[7] Y. Tokura (Ed.), Colossal Magnetoresistive Oxides, 2000. Gordon and Breach, Amsterdam.
[8] M.H. Phan, M.B. Morales, N.S. Bingham, H. Srikanth, C.L. Zhang, S.W. Cheong, Phys. Rev. B 81 (2010) 094413.
[9] M. Uehara, S. Mori, C.H. Chen, S.W. Cheong, Nature 399 (1999) 560.
[10] M. Fath, S. Freisem, A.A. Menovsky, Y. Tomioka, J. Aarts, J.A. Mydosh, Nature 285 (1999) 1540.
[11] Haibiao Zhou, Lingfei Wang, Yubin Hou, Zhen Huang, Qingyou Lu, Wenbin Wu, Nat. Commun. 6 (2015) 8980.
[12] J. Deisenhofer, D. Braak, H.A. Krug von Nidda, J. Hemberger, R.M. Eremina, V.A. Ivanshin, A.M. Balbashov, G. Jug, A. Loidl, T. Kimura, Y. Tokura, Phys. Rev. Lett. 95 (2005) 257202.
[13] A. Shengelaya, Guo-meng Zhao, H. Keller, K.A. Müller, Phys. Rev. Lett. 77 (1996) 5296.
[14] M.T. Causa, M. Tovar, A. Caneiro, F. Prado, G. Ibañez, C.A. Ramos, A. Butera, B. Alascio, X. Obradors, S. Piñol, F. Rivadulla, C. Vázquez-Vázquez, M.A. López-Quintela, J. Rivas, Y. Tokura, S.B. Oseroff, Phys. Rev. B 58 (1998) 3233.
[15] D.L. Huber, M.T. Causa, F. Prado, M. Tovar, S.B. Oseroff, Phys. Rev. B 60 (1999) 12155.
[16] A. Abragam, B. Bleaney, Electron Paramagnetic Resonance of Transition Ions, Clarendon Press, Oxford, 1970.
[17] M. Auslender, E. Rozenberg, A.I. Shames, M. Ya, Mukovskii, J. Appl. Phys. 113 (2013) 17D705.
[18] J. Fan, L. Ling, B. Hong, L. Zhang, L. Pi, Y. Zhang, Phys. Rev. B 81 (2010) 144426.
[19] L. Chen, J. Fan, W. Tong, D. Hu, Y. Ji, J. Liu, L. Zhang, L. Pi, Y. Zhang, H. Yang, Sci. Rep. 6 (2016) 14.
[20] J. Kubler, Theory of Itinerant Electron Magnetism, Clarendon Press, Oxford, 2000.
[21] Hyoungjeen Jeen, Amlan Biswas, Phys Rev B 88 (2013) 024415.
[22] J.P. Joshi, K.V. Sarathy, A.K. Sood, S.V. Bhat, C.N.R. Rao, J. Phys. Condens. Matter 16 (2004) 2869.
[23] V.A. Ryzhov, A.V. Lazuta, O.P. Smirnov, I.A. Kiselev, Yu P. Chernenkov, S.A. Borisov, I.O. Troaynchuk, D.D. Khalyavin, Phys. Rev. B 72 (2005) 134427.
[24] Tapan Chatterji, Bachir Ouladdiaf, P. Mandal, B. Bandyopadhyay, B. Ghosh, Phys. Rev. B 66 (2002) 054403.
[25] A. Shengelaya, Guo-meng Zhao, H. Keller, K. A. Müller, Phys. Rev. B 61 (2000) 5888.
[26] A.I. Shames, E. Rozenberg, W.H. McCarroll, M. Greenblatt, G. Gorodetsky, Phys. Rev. B 64 (2001) 172401.
[27] V. Markovich, I. Fita, A.I. Shames, R. Puzniak, E. Rozenberg, C. Martin, A. Wisniewski, Y. Yuzhelevskii, A. Wahl, G. Gorodetsky, Phys. Rev. B 68 (2003) 094428.
[28] J. Fan, L. Ling, B. Hong, W. Tong, L. Zhang, Y. Shi, W. Zhang, Y. Zhu, D. Hu, Y. Ying, L. Pi, Y. Zhang, Appl. Phys. A 112 (2013) 397.
[29] A. Asamitsu, Y. Tomioka, H. Kuwahara, Y. Tokura, Nature (London) 388 (1997) 50.
[30] K.H. Ahn, T. Lookman, A.R. Bishop, Nature (London) 428 (2004) 401.
[31] M. Jaime, M.B. Salamon, M. Rubinstein, R.E. Treece, J.S. Horwitz, D.B. Chrisey, Phys. Rev. B 54 (1996) 11914.
[32] J.M. De Teresa, K. Dörr, K.H. Müller, L. Schultz, R.I. Chakalova, Phys. Rev. B 58 (1998) R5928.
[33] D.L. Huber, M.S. Seehra, J. Phys. Chem. Solid. 36 (1975) 723.
[34] F. Rivadulla, M.A. López-Quintela, L.E. Hueso, J. Rivas, M.T. Causa, C. Ramos, R.D. Sánchez, M. Tovar, Phys. Rev. B 60 (1999) 11922.
[35] M.T. Causa, G. Alejandro, R. Zysler, F. Prado, A. Caneiro, M. Tovar, J. Magn. Magn Mater. 196 (1999) 506.